Magnetic phase transitions and crystal-field splitting in K_2UX_5 (X=Cl,Br,I)

L. Keller,* A. Furrer, P. Fischer, and P. Allenspach
Laboratorium für Neutronenstreuung, Eidgenössische Technische Hochschule Zürich and Paul Scherrer Institut, CH-5232 Villigen PSI, Switzerland

K. Krämer and H. U. Güdel
Institut für Anorganische, Analytische und Physikalische Chemie, Universität Bern, CH-3000 Bern, Switzerland

A. Dönni
The Institute of Physical and Chemical Research (RIKEN), Wako, Saitama 351-01, Japan

T. Suzuki
Department of Physics, Faculty of Science, Tohoku University, Sendai 980, Japan
(Received 28 July 1994; revised manuscript received 30 September 1994)

A consistent physical analysis of both elastic- and inelastic-neutron-scattering experiments as well as of specific-heat measurements in the temperature range from 7 mK to 295 K on polycrystalline samples of the $5f^3$ electron system K_2UX_5 (X=Cl,Br,I) was performed on the basis of a two-dimensional Ising model. The orthorhombic structure of K_2PrCl_5 type was refined in the paramagnetic state and turned out to be built up by well-separated chains of $[UX_3X_{4/2}]^{2-}$ polyhedra. K_2UCl_5 and K_2UBr_5 undergo a magnetic phase transition to a long-range antiferromagnetically ordered state corresponding to the Shubnikov space group $Pn'm'a'$ with $\mathbf{k}=\mathbf{0}$ at Néel temperatures $T_N=3.8(1)$ K and $T_N=2.8(1)$ K, respectively. K_2UI_5 orders antiferromagnetically at $T_N=1.45(3)$ K in the Shubnikov space group $Pnm'a$ with $\mathbf{k}=\mathbf{0}$. The ordering temperatures, the dominant intrachain exchange interactions, as well as the magnitudes of the magnetic moments at saturation [$\mu_U=3.24(4)\mu_B$, $2.31(4)\mu_B$, and $1.80(4)\mu_B$ for X=Cl, Br, and I, respectively] are strongly dependent on the intra- and interchain uranium distances. Specific-heat measurements showed large magnetic contributions at temperatures higher than T_N for all compounds K_2UX_5 (X=Cl,Br,I). Analyzed in terms of the anisotropic two-dimensional Ising model, these measurements proved the existence of short-range magnetic ordering along the uranium chains above T_N, followed by the long-range ordered magnetic phase. By means of inelastic neutron scattering we determined the crystal-field splitting of the series K_2UX_5 (X=Cl,Br,I) from well-defined crystal-field peaks. Due to the low local symmetry at the uranium site (sevenfold coordination), the crystal-field level scheme was analyzed introducing geometrical dependences of crystal-field parameters which provide a good description of both crystal-field energy levels and transition probabilities.

I. INTRODUCTION

The study of magnetic ordering phenomena in uranium (III) halides has for many years been subject of several, mostly bulk magnetic investigations. However, magnetic structure determinations applying neutron-scattering techniques have so far only been carried out for binary halides UX_3, such as UCl_3,[1,2] UBr_3,[2,3] and UI_3.[4] In Ref. 1 the magnetic properties of UCl_3 were interpreted on the basis of uranium chains with predominant antiferromagnetic intrachain and weaker interchain interaction. Schmid *et al.* reported on one-dimensional spin-wave excitations in UX_3 (X=Cl,Br) observed by means of neutron spectroscopic investigations.[2]

The aim of this work is the investigation of magnetic behavior of uranium chain systems. Compounds with well-separated chains may act as model systems for the investigation of intra- and interchain interactions and therefore for the investigation of the short- and long-range magnetic ordering phenomena in predominantly low-dimensional systems.

Ternary halides K_2UX_5 (X=Cl,Br,I) of uranium are nonmetallic $5f^3$ electron systems with a $^4I_{9/2}$ ground state of the U^{3+} ions. These compounds crystallize in the orthorhombic K_2PrCl_5-type structure corresponding to space group $Pnma$.[5,6] The structure may be thought as a stacking of well-separated chains of $[UX_3X_{4/2}]^{2-}$ polyhedra which are connected over rather large potassium contacts. Bulk magnetic measurements of the chlorides A_2UCl_5 (A=K,NH_4,Rb) (Ref. 7) give evidence for antiferromagnetic ordering. However, a first attempt to determine the magnetic structure of K_2UCl_5 (Ref. 8) was not successful because of limited sample quality. Recently, the magnetic ordering of K_2UBr_5 was investigated.[9] Neutron-diffraction experiments reveal a long-range magnetically ordered phase below $T_N=2.8(1)$ K, whereas measurements of the bulk magnetic susceptibility give evidence for low-dimensional magnetic ordering at temperatures higher than T_N.

Here we report on a consistent physical interpretation

of magnetic interactions, magnetic phase transitions, magnetic phases, and crystal-field effects in the uranium chain compounds K_2UX_5 (X=Cl,Br,I), based both on elastic- and inelastic-neutron-scattering experiments, measurements of the specific heat, and on a two-dimensional Ising model. The predominantly chemical aspects of the investigations are summarized in a recent review.[10]

II. EXPERIMENT

Neutron-diffraction experiments were performed with use of the multidetector powder diffractometer DMC (Ref. 11) and the two-axis diffractometer 2AX at the reactor Saphir in Villigen. An "ILL-type" helium gas-flow cryostat was used for temperatures above 1.5 K. The powder samples were enclosed under a He gas atmosphere into cylindrical V tubes of 8 mm diameter and 50 mm height. Down to 7 mK a standard Oxford dilution ^{3}He/^{4}He refrigerator was used and the powder samples were enclosed within a cylindrical Cu container of 8 mm diameter, which allowed condensation of liquid ^{4}He into the sample for optimal thermal contact. For the investigation of the magnetic ordering of K_2UX_5 (X=Cl,Br,I) the neutron-diffraction measurements were performed on DMC in the high intensity mode with neutron wavelength $\lambda=1.7037$ Å obtained from a vertically focusing Ge (3,1,1) monochromator. All DMC measurements were corrected for absorption according to the measured transmission: $\mu=0.395$ cm^{-1} (K_2UCl_5), $\mu=0.363$ cm^{-1} (K_2UBr_5), and $\mu=0.168$ cm^{-1} (K_2UI_5). The magnetic structures of the ordered states were calculated by a standard Rietveld program.[12] For the calculations the neutron-scattering lengths published by Sears[13] and a calculated relativistic neutron magnetic form factor for U^{3+} (Ref. 14) were used. The temperature dependences of the strongest magnetic Bragg peaks were determined on the two-axis diffractometer 2AX.

Inelastic-neutron-scattering experiments were carried out for polycrystalline samples of K_2UX_5 (X=Cl,Br,I) with use of the three-axis spectrometers 3AX and MARC at the reactor Saphir in Villigen. The energy of the scattered neutrons was fixed at 15 meV, and a pyrolytic graphite filter was used to reduce higher-order contamination. Energy spectra were taken at various temperatures and moduli of the scattering vector **Q** for energy transfers up to 80 meV.

The measurements of the specific heat were performed by the adiabatic technique at Tohoku University, Sendai. In order to guarantee optimal thermal contact, the powder samples were pressed in pellets and mounted on a Cu plate. The temperature range from 0.7 to 40 K was covered using ^{3}He and ^{4}He gas-flow cryostats.

III. NEUTRON-DIFFRACTION ANALYSIS

The compounds K_2UX_5 (X=Cl,Br,I) belong to the K_2PrCl_5-type structure (orthorhombic space group *Pnma*, $Z=4$). Details of the results of the structure refinement in the paramagnetic state are published elsewhere.[9,10,15] The lattice and positional (for the Cl and I compounds) parameters and the shortest intra- and interchain distances are summarized in Tables I–III. K_2UX_5 contains chains of $[UX(1)X(2)X(3)X(4)_{4/2}]^{2-}$ polyhedra parallel to the b axis with sevenfold coordinated U^{3+} (distorted pentagonal bipyramides; Fig. 1). The chains are well separated from each other by potassium ions.

TABLE I. Crystallographic and magnetic data of K_2UX_5 (X=Cl,Br,I). a,b,c: lattice constants at $T\leq 20$ K, $d_{U\text{-}U}$: uranium distances, T_N: Néel temperature, **k**: magnetic propagation vector, μ_U: ordered magnetic moment/U^{3+} at saturation.

	K_2UCl_5	K_2UBr_5 (Ref. 9)	K_2UI_5
a (Å)	12.6156(7)	13.212(1)	14.204(9)
b (Å)	8.7636(5)	9.1642(7)	9.805(6)
c (Å)	7.9365(4)	8.3619(6)	9.040(6)
$d_{U\text{-}U}$ (Å) intrachain	4.556(3)	4.782(3)	5.14(1)
$d_{U\text{-}U}$ (Å) interchain	6.873(4)	7.184(5)	7.70(1)
T_N (K)	3.8(1)	2.8(1)	1.45(3)
k	(0,0,0)	(0,0,0)	(0,0,0)
Magn. space group	*Pn'm'a'*	*Pn'm'a'*	*Pnm'a*
μ_U (μ_B)	3.24(4)	2.31(4)	1.80(4)

In powder neutron-diffraction experiments a long-range magnetic ordering causes additional Bragg peaks below T_N due to the antiferromagnetic superstructure. The difference of the diffraction data below T_N and above T_N therefore contains to a good approximation the information on the magnetic structure only. Figure 2(a) shows the difference pattern I(1.5 K)-I(4.2 K) of K_2UCl_5 which was refined by means of a Rietveld program for DMC data. All magnetic Bragg peaks may be indexed in terms of the nuclear cell, i.e., the magnetic propagation vector $\mathbf{k}=\mathbf{0}$. For the fit procedure the magnetic contributions to the scattering pattern were included up to $2\Theta=40°$ ($\lambda=1.7037$ Å). The best fit of calculated and observed pattern was achieved for the Shubnikov space group *Pn'm'a'*. The uranium ions occupy the special site (4*c*) with site symmetry (.*m*.) in *Pnma*. In *Pn'm'a'* the symmetry of site (4*c*) changes to an antimirror plane (.*m'*.) with the result that the magnetic moments have only components along the *a* and *c* axes. The refinement of the magnetic structure results in an ordered magnetic moment of $3.24(4)\mu_B/U^{3+}$ with components $\mu_x=2.32(4)\mu_B$ and $\mu_z=2.27(4)\mu_B$ which are equal within the error limits. The magnetic moments of the four uranium ions per unit cell are summarized in Table II. The U^{3+} chains parallel to the *b* axis, which consist of U(1)-U(3) resp. U(2)-U(4), are ordered antiferromagnetically. The magnetic moments of neighboring chains, i.e., U(1)-U(3) versus U(2)-U(4), are perpendicular to each

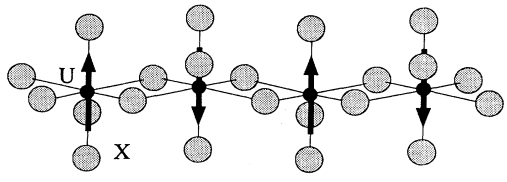

FIG. 1. Chain of uranium polyhedra $[UX(1)X(2)X(3)X(4)_{4/2}]^{2-}$ of K_2UX_5 along [010].

TABLE II. K_2UCl_5: coordinates (determined in the paramagnetic state at $T=20$ K) and components of the ordered magnetic moment of U^{3+} derived from the difference pattern 1.5–4.2 K. Shubnikov space group $Pn'm'a'$, $\mathbf{k}=0$, $\mu_U=3.24(4)\mu_B$.

K_2UCl_5	x/a	y/b	z/c	μ_x (μ_B)	μ_y (μ_B)	μ_z (μ_B)
U(1)	0.5064(4)	0.25	0.0780(6)	2.32(4)	0	2.27(5)
U(2)	0.9936	0.75	0.5780	−2.32	0	2.27
U(3)	0.4936	0.75	0.9220	−2.32	0	−2.27
U(4)	0.0064	0.25	0.4220	2.32	0	−2.27
K (8*d*)	0.6715(6)	0.496(1)	0.5574(9)			
Cl1 (4*c*)	0.9948(4)	0.75	0.9328(5)			
Cl2 (4*c*)	0.7906(3)	0.25	0.3280(6)			
Cl3 (4*c*)	0.6809(3)	0.25	0.8652(5)			
Cl4 (8*c*)	0.5815(2)	0.5442(3)	0.1682(4)			

other within the error limits. The overall magnetic moment of the unit cell disappears because of the antiferromagnetic intrachain coupling. The long-range antiferromagnetic ordering of K_2UCl_5 is similar to the ordering observed in K_2UBr_5.[9] Nevertheless, the ordered magnetic moments in the chloride are remarkably enlarged compared to the value of the bromide.

The analysis of the difference neutron-diffraction pattern of K_2UI_5 (Fig. 3) showed that also in the case of the iodide the magnetic unit cell is equal to the chemical unit cell, i.e., $\mathbf{k}=\mathbf{0}$. However the refinement of the magnetic structure unambiguously revealed that K_2UI_5 orders antiferromagnetically corresponding to another Shubnikov space group $Pnm'a$, in contrast to the Shubnikov space group $Pn'm'a'$ of the Cl and Br compounds. These two magnetic space groups are closely related. In $Pnm'a$ the symmetry of the site (4*c*) is also an antimirror plane (.*m'*.) i.e., $\mu_y=0$. The only difference is a rotation of the magnetic moments of the chain U(2)-U(4) by 180°. This leads to a change of the relative intensities of the magnet-

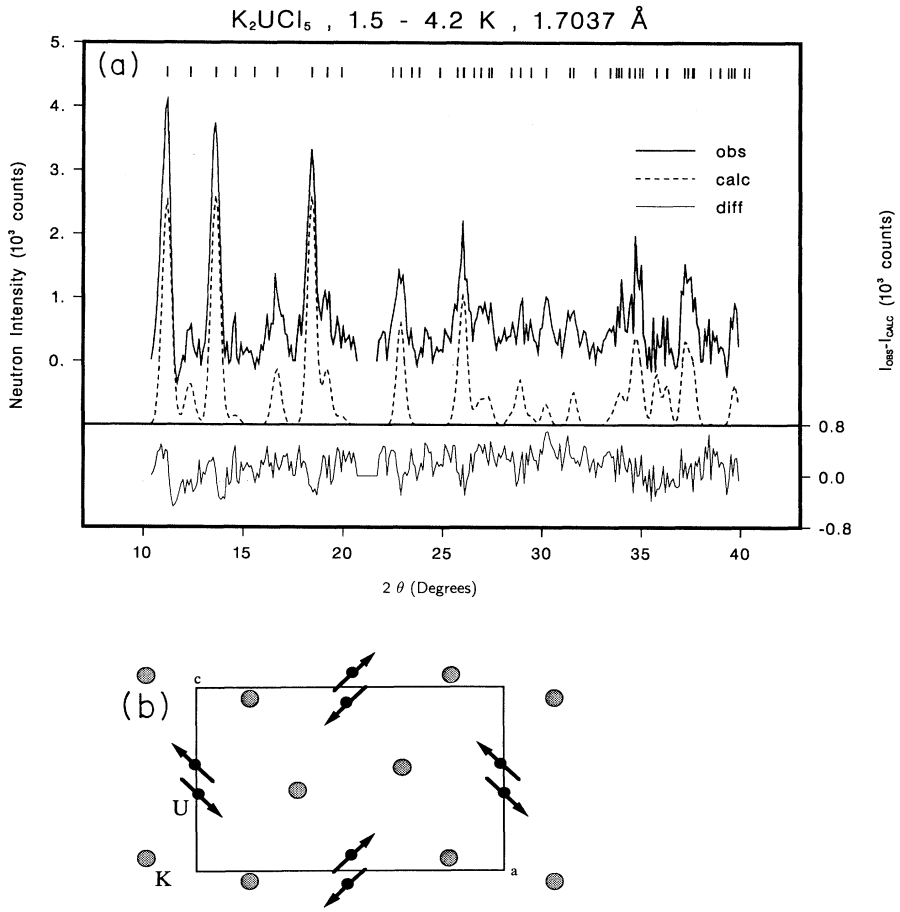

FIG. 2. (a) Observed and calculated neutron-diffraction pattern 1.5–4.2 K (DMC, high intensity mode, $\lambda=1.7037$ Å) of K_2UCl_5. (b) Antiferromagnetic structure of K_2UCl_5, associated with magnetic moments due to U^{3+} ions.

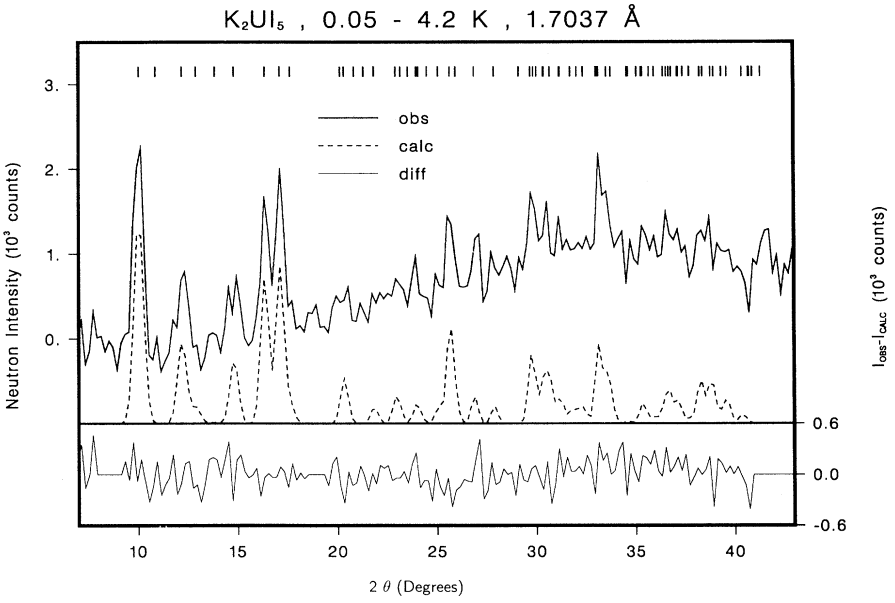

FIG. 3. Observed and calculated neutron-diffraction pattern 50 mK–4.2 K (DMC, high intensity mode, $\lambda = 1.7037$ Å) of K_2UI_5.

ic peaks and may be easily distinguished in neutron-diffraction experiments. The ordered magnetic moments in K_2UI_5 turned out to be $1.82(4)\mu_B/U^{3+}$ with components $\mu_x = 0.95(3)\mu_B$ and $\mu_z = 1.50(4)\mu_B$ (Table III). The results of the magnetic structure determination of the compounds K_2UX_5 (X=Cl,Br,I) are summarized in Table I. The ordering temperatures as well as the magnitudes of the magnetic moments at saturation are strongly dependent on the intra- and interchain uranium distances. In particular the Néel temperatures show a linear increase with decreasing uranium distances.

IV. SPECIFIC-HEAT ANALYSIS: LONG- AND SHORT-RANGE MAGNETIC ORDERING

Neutron powder-diffraction experiments are a powerful and useful tool to investigate long-range magnetic ordering phenomena, whereas a direct proof of short-range one-dimensional magnetic ordering requires quasielastic neutron scattering on single crystals, as the magnetic intensity is distributed over planes in reciprocal space.[16] In order to investigate the magnetic behavior of polycrystalline samples above and around T_N, measurements of the specific heat were performed. In Fig. 4 we show $C_p(T)$ for K_2UX_5 (X=Cl,Br,I) as a function of the applied magnetic field. In all three compounds, the zero-field peak position corresponds to the Néel temperatures T_N determined in neutron-scattering experiments and shows the phase transition to a magnetically long-range ordered state. The external magnetic field shifts T_N towards lower temperatures and the peak smoothes out. The spontaneous magnetic structure is distorted by the induced ferromagnetic component and may be shifted below the range of observation. In order to remove the lattice contribution and to obtain the magnetic part only, a Debye law was fitted to the data and subtracted. The resulting Debye temperatures are $\Theta_D \approx 150$ K (K_2UCl_5), 100 K (K_2UBr_5), and 80 K (K_2UI_5), which are in the range of values for uranium compounds found in the literature ($\Theta_D \approx 200$ K).

The magnetic specific heat ΔC of K_2UX_5 (X=Cl,Br,I) is shown in Fig. 5. There is a broad peak above T_N, followed by the narrow anomaly at T_N. The magnetic entropy $S(T)$ may be obtained by integrating

TABLE III. K_2UI_5: coordinates (determined in the paramagnetic state at $T=4.2$ K) and components of the ordered magnetic moment of U^{3+} derived from the difference pattern 50 mK–4.2 K. Shubnikov space group $Pnm'a$, $\mathbf{k}=0$, $\mu_U = 1.80(4)\mu_B$.

K_2UI_5	x/a	y/b	z/c	μ_x (μ_B)	μ_y (μ_B)	μ_z (μ_B)
U(1)	0.508	0.25	0.086	0.95(3)	0	1.50(4)
U(2)	0.992	0.75	0.586	0.95	0	−1.50
U(3)	0.492	0.75	0.914	−0.95	0	−1.50
U(4)	0.008	0.25	0.414	−0.95	0	1.50
K (8*d*)	0.680(3)	0.488(5)	0.557(5)			
I1 (4*c*)	0.998(5)	0.75	0.940(5)			
I2 (4*c*)	0.785(3)	0.25	0.340(5)			
I3 (4*c*)	0.688(3)	0.25	0.855(5)			
I4 (8*c*)	0.579(2)	0.547(2)	0.179(3)			

$S(T)=\int_0^T C(\tau)/\tau d\tau$, e.g., for K_2UCl_5. From Fig. 6 it is evident that the cooperative phase transition only releases about 10% of R ln2, the expected molar entropy for a doublet ground state. The total entropy of R ln2=5.76 J/mol K is obviously only recovered if the temperature is raised above 30 K.

The zero-field data ΔC were analyzed in terms of the well-known Onsager solution[17] of the anisotropic two-dimensional Ising model (solid lines in Fig. 5). In this model the exchange parameters J_1 and J_2 and the Néel temperature T_N are related by

$$1=\sinh\left[\frac{2J_1}{k_B T_N}\right]\sinh\left[\frac{2J_2}{k_B T_N}\right]. \quad (1)$$

Fixing T_N at the experimentally determined value, we are left with only one free parameter. The solid lines in Fig. 5 are the best fits of this model to the data and show excellent agreement. The resulting parameters are summarized in Table IV. There is a large anisotropy of the exchange interaction. The magnitude of the intrachain

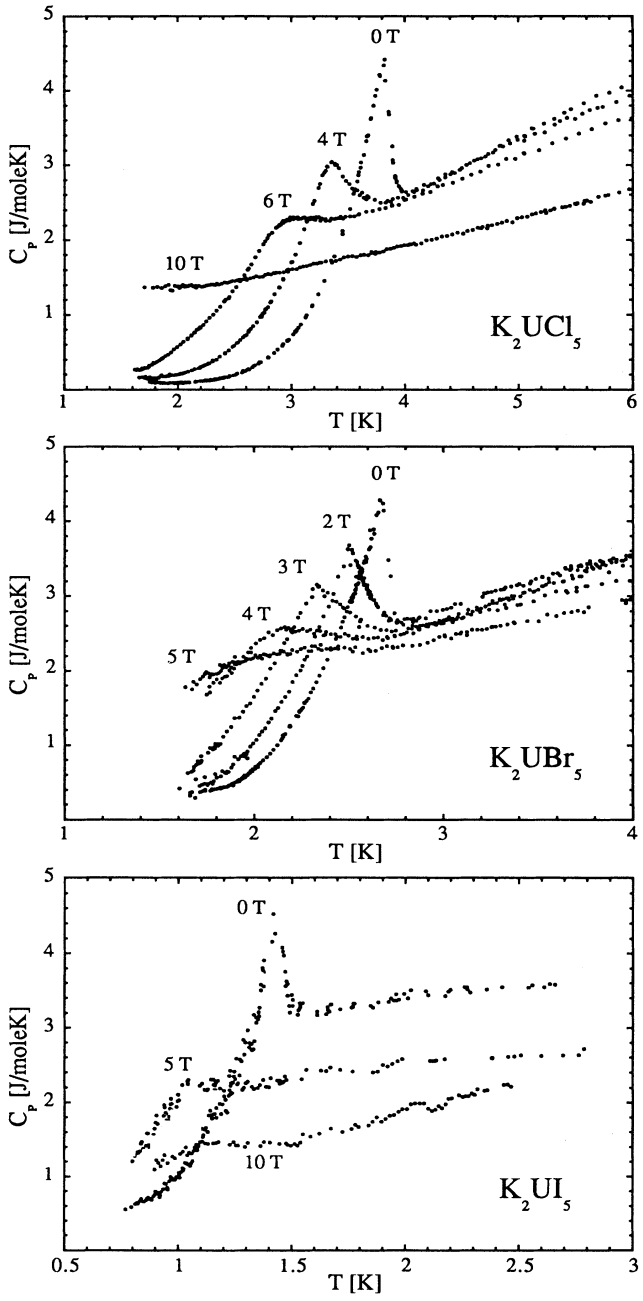

FIG. 4. K_2UX_5 (X=Cl,Br,I): Specific heat $C_p(T)$ as a function of the applied magnetic field.

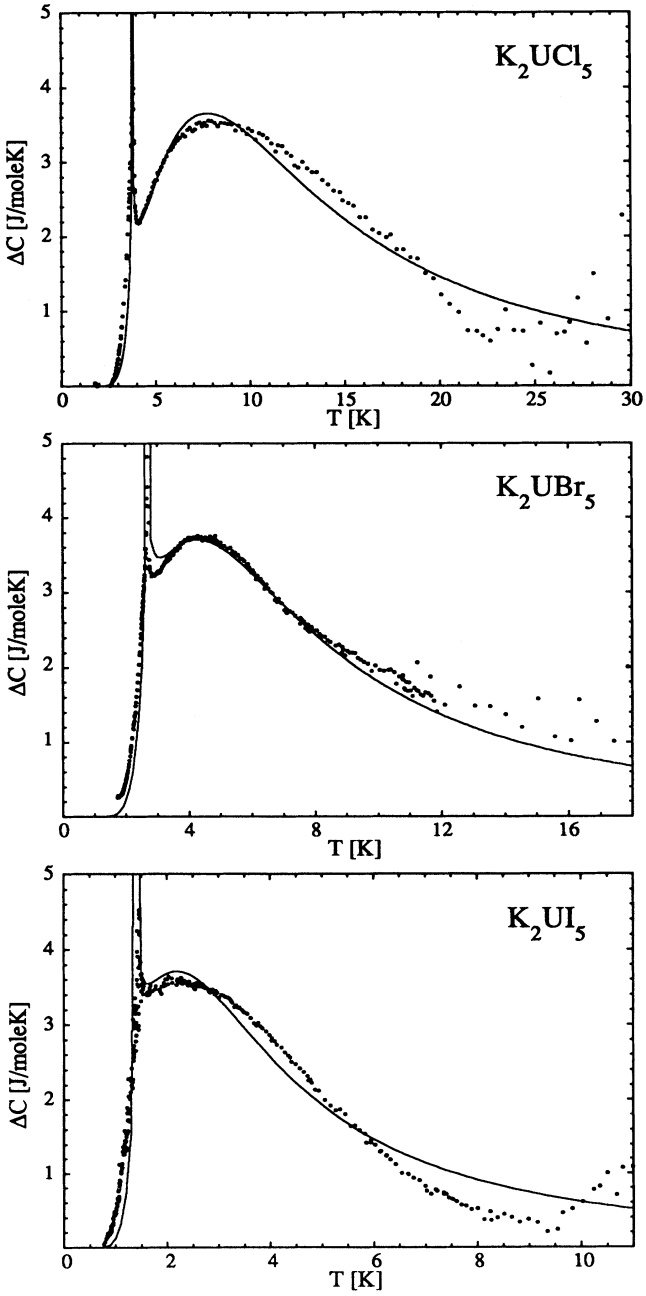

FIG. 5. K_2UX_5 (X=Cl,Br,I): Magnetic contribution ΔC to the specific heat. The solid lines are model calculations as described in the text.

TABLE IV. K_2UX_5 (X=Cl,Br,I): Coupling parameters J_1,J_2 and Néel temperature T_N derived by a fit of the anisotropic two-dimensional Ising model to the specific-heat data.

	J_1 (K)	J_2 (K)	T_N (K)
K_2UCl_5	−9.3(2)	−0.04(1)	3.8(1)
K_2UBr_5	−5.4(2)	−0.04(1)	2.8(1)
K_2UI_5	−2.85(5)	−0.03(1)	1.45(5)

parameter J_1 turns out to be two orders of magnitude bigger than the interchain parameter J_2, which again reflects the chemical chain structure. The dominant coupling along the uranium chains leads to a short-range one-dimensional magnetic ordering which is shown by the broad anomalies in Fig. 5. The maximum of this peak essentially corresponds to the strength of the intrachain coupling J_1. The interchain coupling J_2 acts as a distortion and leads to the long-range magnetic ordering indicated by the sharp peak at T_N and confirmed by the neutron-diffraction experiments described above.

Since no closed-form expressions for the behavior of the specific heat in an external magnetic field exist, a Padé approximation for T_N versus H introduced by Bienenstock[18] was used to explain the data in Fig. 4. According to this approximation the antiferromagnetic ordering temperature T_N varies as a function of external magnetic field H as follows:

$$\frac{T_N(H)}{T_N(0)}=\left[1-\left[\frac{H}{H_c}\right]^2\right]^{\xi}, \tag{2}$$

where $H_c=-zJ/\mu$ and $\xi=0.87$ (calculated for a square lattice but mainly depending on the dimensionality). z denotes the coordination number, J the (isotropic) exchange parameter, and μ the magnetic moment. For the fit with J as the fitting parameter $z=4$ and for μ the values in Table I were chosen. The results of the fits for

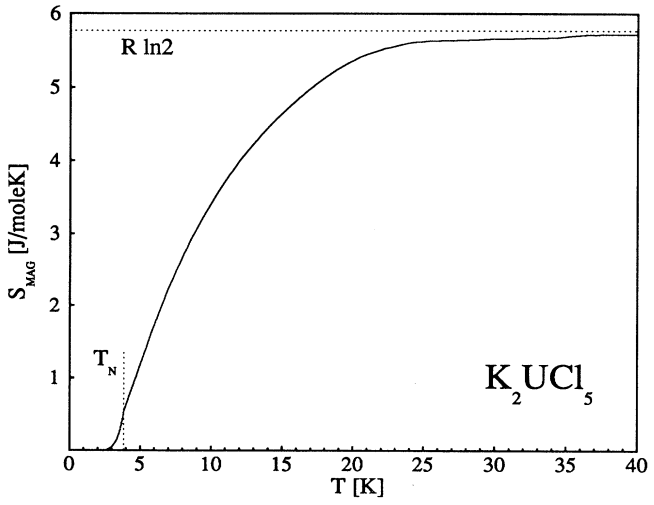

FIG. 6. K_2UCl_5: Temperature dependence of the magnetic entropy $S(T)$.

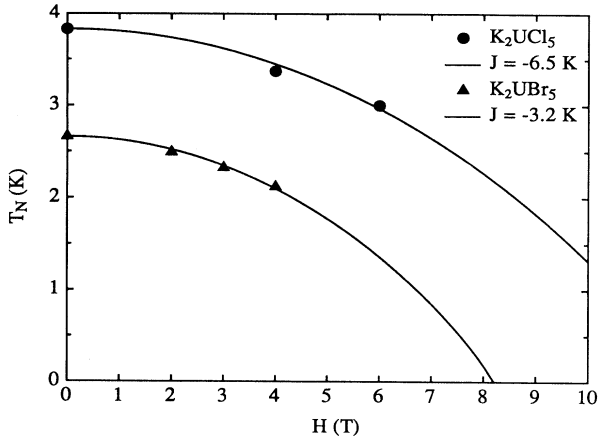

FIG. 7. Padé approximation (lines) of the magnetic-field dependence of T_N for K_2UCl_5 and K_2UBr_5. The errors in T_N are for high magnetic fields in the order of the symbol sizes.

K_2UCl_5 and K_2UBr_5 are shown in Fig. 7, yielding $J=-6.5$ K and $J=-3.2$ K, respectively. Since powder averaging and anisotropy are not included in this approximation, the agreement with the values obtained with the anisotropic two-dimensional Ising model (Table IV) can be regarded as very good.

V. INELASTIC-NEUTRON-SCATTERING ANALYSIS OF THE CRYSTAL-FIELD SPLITTING

The crystal-field Hamiltonian for the symmetry of U^{3+} in K_2UX_5 (X=Cl,Br,I) is given by

$$H_{\mathrm{CEF}}=\sum_{n=2,4,6}\sum_{m=0}^{n} B_n^m O_n^m , \tag{3}$$

where the B_n^m denote the crystal-field parameters and the O_n^m are operator equivalents built up by spin operators.[19] The lack of point symmetry at the uranium site (sevenfold coordination) leads to 15 independent nonzero crystal-field parameters. Equation (3) gives rise to a decomposition of the ground-state multiplet $^4I_{9/2}$ of the U^{3+} ions into five Kramers doublets. Thus it is impossible to derive the 15 independent crystal-field parameters of Eq. (3) from the energies of the crystal-field states alone. However, from general experience with crystal-field problems for a large group of compounds the ratios of the parameters B_n^m for a particular degree n are found to be reasonably determined by taking account of the nearest-neighbor polyhedron:

$$B_n^m=\frac{\gamma_n^m}{\gamma_n^0}B_n^0 . \tag{4}$$

The geometrical coordination factors γ_n^m as defined, e.g., by Hutchings[20] can easily be calculated from the structural data.

Recently, the crystal-field level schemes of diluted compounds K_2LaX_5/U^{3+} (X=Cl,Br,I) have been determined by means of optical luminescence experiments.[21] Our analysis of the level scheme in terms of Eqs. (3) and

(4) revealed that there is not a unique set of crystal-field parameters to describe the level scheme alone, i.e., transition probabilities have to be taken into account. In order to get accurate information on crystal-field energies and intensities, we have performed inelastic-neutron-scattering experiments of K_2UX_5 (X=Cl,Br,I).

Typical spectra obtained for K_2UBr_5 are shown in Fig. 8. There are three well resolved inelastic lines at -7.5, -14.5, and -19 meV, each of which exhibits a different behavior as a function of temperature and scattering vector. The intensities of crystalline electric-field (CEF) transitions are decreasing with increasing scattering vector Q due to the magnetic form factor, and their temperature dependences are governed by Boltzmann statistics, whereas phonon intensities usually increase with increasing scattering vector (apart from the modulation due to the structure factor) and their temperature dependences follow Bose statistics. Therefore we can unambiguously attribute the lines at -7.5 and -14.5 meV to ground-state CEF transitions whereas the line at -19 meV is identified as a phonon excitation. These results are in agreement with optical investigations on diluted samples in which the excited CEF levels were found at 7.44, 14.01, 28.76, and 48.73 meV.[21] No further inelastic excitations were detected up to an energy transfer ΔE of -80 meV, i.e., transition probabilities for additional CEF transitions must be small. The analysis of the temperature dependences of the inelastic intensities in terms of Boltzmann statistics revealed that the additional CEF levels are not expected to lie below 25 meV.

Similar experiments were performed for K_2UCl_5 (Fig. 9). Again two ground-state CEF transitions were observed ($\Delta E=-9.9$ and -18.9 meV, respectively). Due to the large nuclear-scattering length of Cl, the spectra at high temperatures T and high scattering vectors Q show a significant increase of the background and additional phonon excitations. Typical spectra for K_2UI_5 are shown in Fig. 10. At $\Delta E=-4.7$ meV we observe a ground-state CEF transition. The line at an energy transfer of about -11 meV is composed of two excitations. Due to their temperature dependences they can be identified as a ground-state CEF and a phonon excitation. The linewidth of the peak around -20 meV is unusually large and indicates that several excitations which are accidentally degenerated may lead to this line.

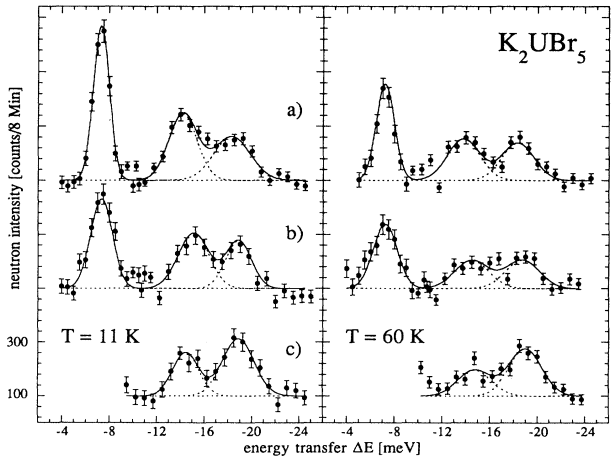

FIG. 8. Energy spectra of neutrons scattered from polycrystalline K_2UBr_5 at $T=11$ K (left part) and $T=60$ K (right part). (a) $Q=2$ Å^{-1}, (b) $Q=3$ Å^{-1}, (c) $Q=4.2$ Å^{-1}.

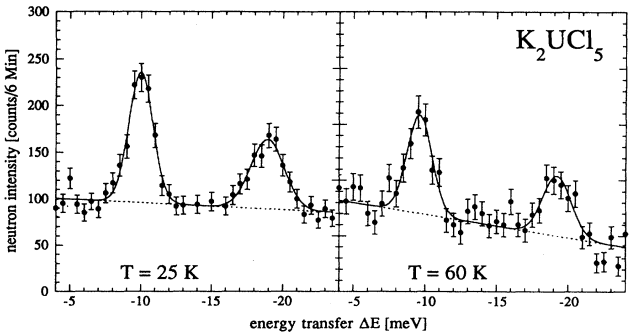

FIG. 9. Energy spectra of neutrons scattered from polycrystalline K_2UCl_5 ($Q=2$ Å^{-1}) for $T=25$ K and $T=60$ K.

Using the geometrical constraints according to Eq. (4) we are left with three independent parameters B_2^0, B_4^0, B_6^0, which we have least-squares fitted to the observed spectra in a first step. Following Lea, Leask, and Wolf[22] we introduced the parametrization

$$B_2^0=\frac{1}{F_2}W(1-|y|)\ ,$$
$$B_4^0=\frac{1}{F_4}Wxy\ , \tag{5}$$
$$B_6^0=\frac{1}{F_6}W(1-|x|)y\ ,$$

with $F_2=2$, $F_4=60$, $F_6=2520$, $-1\le x,y\le 1$, and W is a scale factor. Equation (5) corresponds to the most general combination of second-, fourth-, and sixth-order CEF parameters. For only one parameter set x,y reasonable agreement between the observed and calculated energies and intensities was obtained. Then we have also allowed the parameters B_2^1 and B_2^2 to vary independently, whereas the remaining crystal-field parameters were

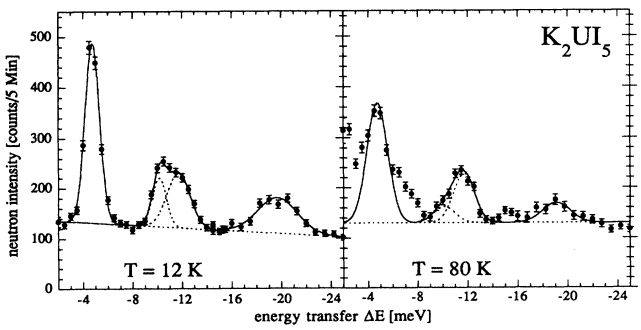

FIG. 10. Energy spectra of neutrons scattered from polycrystalline K_2UI_5 ($Q=2$ Å^{-1}) for $T=12$ K and $T=80$ K.

TABLE V. Crystal-field parameters of K_2UX_5 (X=Cl,Br,I). The values of B_2^0, B_2^1, B_2^2, B_4^0, and B_6^0 are results of a mean-square fit, B_n^m/B_n^0 is given by Eq. (4).

	K_2UCl_5	K_2UBr_5	K_2UI_5
B_2^0 (meV)	−0.27(2)	−0.20(2)	−0.10(2)
B_2^1 (meV)	1.00(2)	0.97(2)	0.99(2)
B_2^2 (meV)	0.62(3)	0.54(3)	0.42(3)
B_4^0 (meV)	$-1.01(1)\times10^{-3}$	$-0.81(1)\times10^{-3}$	$-0.56(1)\times10^{-3}$
B_6^0 (meV)	$-0.56(5)\times10^{-4}$	$-0.50(5)\times10^{-4}$	$-0.38(5)\times10^{-4}$
B_4^1/B_4^0	11.29	11.44	10.63
B_4^2/B_4^0	4.48	2.45	0.99
B_4^3/B_4^0	−219.82	−182.63	−161.41
B_4^4/B_4^0	24.06	22.66	20.98
B_6^1/B_6^0	−1.14	−1.65	−1.99
B_6^2/B_6^0	−2.06	−2.52	−2.62
B_6^3/B_6^0	0.90	0.62	0.59
B_6^4/B_6^0	−0.41	−0.83	−1.06
B_6^5/B_6^0	4.49	7.24	10.04
B_6^6/B_6^0	13.02	14.22	16.89

again fixed at the geometrical coordination values mentioned above. The procedure converged to a modified set of parameters which, however, did not deviate significantly from the values obtained in the first step. Thus our parametrization can undoubtedly be considered to be a unique solution. We independently analyzed the crystal field of the chloride, bromide, and iodide. The resulting parameters show a systematic dependence on the halide and therefore on the uranium distances (Table V). The calculated and observed crystal-field energies and transition probabilities are compared in Table VI.

The CEF parameters may now be used to calculate the magnetic properties of K_2UX_5 (X=Cl,Br,I). The magnetic single-ion susceptibility turns out to be extremely anisotropic. From a mean-field calculation the ordered magnetic moment lies in the a,c plane without any component along b, which is in agreement with the results of the elastic-neutron-scattering experiments. The mean-field values of the ordered magnetic moments at saturation partly deviate from the experimentally deduced value. For K_2UCl_5 we calculate $1.7\mu_B$ (observed $3.2\mu_B$), for K_2UBr_5 $1.8\mu_B$ (observed $2.3\mu_B$) and for K_2UI_5 $2.0\mu_B$ (observed $1.8\mu_B$). This indicates that we are not dealing with a mean-field system and the pronounced low dimensionality should be taken into account.

The analysis of the crystal-field level scheme of systems without a center of point symmetry at the site of the magnetic ion usually fails due to the large number of indepen-

TABLE VI. Calculated and observed CEF energy levels ΔE and transition intensities for K_2UCl_5, K_2UBr_5, and K_2UI_5. INS: inelastic neutron scattering, Lum.: luminescence measurements.

CEF level	ΔE (calc)	ΔE (obs) INS	ΔE (obs) Lum.	CEF transition	Int. (calc)	Int. (obs) INS
			(K_2UCl_5)			
B	9.44	9.6(3)	9.30	$A\rightarrow B$	1.00	1.0(1)
C	18.69	18.9(3)	17.85	$A\rightarrow C$	0.67	0.7(1)
D	36.18		36.08	$A\rightarrow D$	0.08	
E	58.95		59.14	$A\rightarrow E$	0.05	
			(K_2UBr_5)			
B	7.47	7.5(2)	7.44	$A\rightarrow B$	1.00	1.00(4)
C	14.49	14.5(3)	14.01	$A\rightarrow C$	0.72	0.56(6)
D	28.95		28.76	$A\rightarrow D$	0.08	
E	48.61		48.73	$A\rightarrow E$	0.05	
			(K_2UI_5)			
B	4.63	4.7(1)	4.59	$A\rightarrow B$	1.00	1.00(2)
C	10.00	10.2(4)	10.29	$A\rightarrow C$	0.66	0.3(1)
D	20.22	19.9(5)	21.08	$A\rightarrow D$	0.10	0.3(3)
E	36.18		36.58	$A\rightarrow E$	0.06	

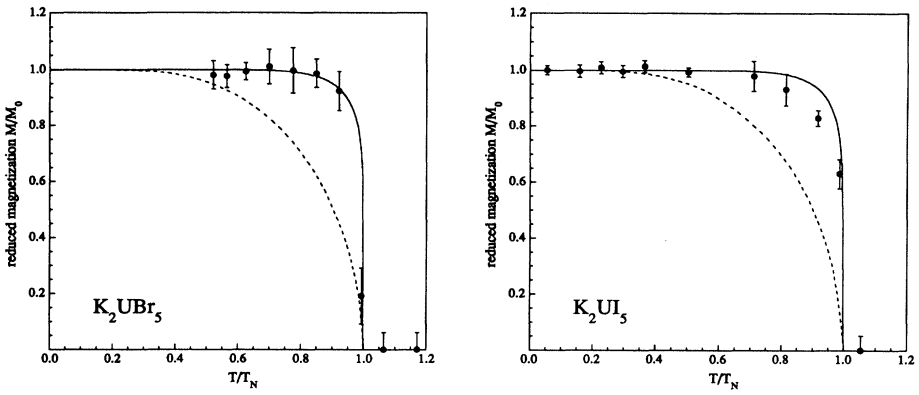

FIG. 11. Temperature dependence of the spontaneous magnetization of K_2UI_5 and K_2UBr_5. The dashed lines denote a mean-field calculation on the basis of the CEF parameters, the solid lines are the results of the two-dimensional anisotropic Ising model with use of the parameters of Table IV.

dent and nonzero crystal-field parameters. Due to the use of experimental results of neutron spectroscopic and optical measurements and the introduction of geometrical coordination factors, which lead to a drastic reduction of independent crystal-field parameters, we found a unique and reasonable solution of the crystalline electric field of K_2UX_5.

VI. DISCUSSION AND SUMMARY

We have presented a consistent physical analysis of the magnetic interactions and magnetic ordering phenomena as well as of crystal-field effects in the uranium chain compounds K_2UX_5 (X=Cl,Br,I) on the basis of a two-dimensional Ising model. The application of various complementary experimental methods, like elastic and inelastic neutron scattering and measurements of the specific heat, leads to a consistent picture of the magnetic phases and the crystalline electric field as well. The key to the understanding of the magnetic properties lies in the chemical chain structure of these compounds and therefore in the interplay of intra- and inter-chain interactions and the resulting anisotropy of the system. Due to the dominant intrachain coupling, short-range one-dimensional ordering occurs at temperatures of approximately $10T_N$ which releases almost 90% of the magnetic entropy in the range down to T_N. At the Néel temperature T_N the interchain interaction drives the system to a long-range three-dimensional ordered magnetic state. Neutron-scattering investigations revealed that the chloride and the bromide order in a similar way whereas the iodide adopts a different but very closely related antiferromagnetic structure. This is presumably due to a slight decrease of the ratio of inter- and intrachain uranium distances: $d_{\text{inter}}/d_{\text{intra}}=1.509$ (K_2UCl_5), 1.502 (K_2UBr_5), and 1.498 (K_2UI_5). In all three compounds we find a linear dependence of the Néel temperature T_N on the intra- and interchain distances. T_N and the ordered magnetic moment of the ion U^{3+} decrease along the series Cl, Br, I.

The temperature behavior of the spontaneous magnetization is very sensitive to the dimensionality and the type of interaction, expressed by the value of the critical parameter β. The applicability of the parameters listed in Table IV to the measurements of the temperature dependence of the magnetic moment derived by neutron-scattering experiments is therefore a crucial test of our model. In Fig. 11 we compare the experimental points of K_2UBr_5 and K_2UI_5 with the results of the two-dimensional Ising model (corresponding to the parameters of Table IV, yielding the critical exponent $\beta=0.125$) and a mean-field calculation ($\beta=0.5$) on the basis of the crystalline electric-field parameters (Table V). The agreement with the former model is obvious and shows that K_2UX_5 acts as an effective two-dimensional Ising system.

ACKNOWLEDGMENTS

Stimulating discussions with J. Mesot are gratefully acknowledged. For financial support we thank the Swiss National Science foundation. Expert help in the operation of the dilution refrigerator was provided by S. Fischer.

*Present address: Department of Chemistry, Stanford University, Stanford, CA 94305.

[1]A. Murasik, P. Fischer, A. Furrer, and W. Szczepaniak, J. Phys. C **18**, 2909 (1985).
[2]B. Schmid, A. Murasik, P. Fischer, A. Furrer, and B. Kanellakopulos, J. Phys. Condens. Matter **2**, 3369 (1990).
[3]A. Murasik, P. Fischer, A. Furrer, B. Schmid, and W. Szczepaniak, J. Less-Common Met. **121**, 151 (1986).
[4]A. Murasik, P. Fischer, and W. Szczepaniak, J. Phys. C **14**, 1847 (1981).
[5]G. Meyer, H.-Chr. Gaebell, and R. Hoppe, J. Less-Common Met. **93**, 347 (1983).
[6]K. Krämer, Ph.D. thesis, Universität Giessen, 1991.
[7]J. Drozdzynski and D. Miernik, Inorg. Chim. Acta **30**, 185 (1978).
[8]P. Fischer and A. Murasik (unpublished).
[9]K. Krämer, L. Keller, P. Fischer, B. Jung, N. N. Edelstein, H. U. Güdel, and G. Meyer, J. Solid State Chem. **103**, 152 (1993).
[10]K. Krämer, H. U. Güdel, G. Meyer, T. Heuer, N. N. Edelstein, B. Jung, L. Keller, P. Fischer, E. Zych, and J. Drozdzynski, Z. Anorg. Allg. Chem. **620**, 1339 (1994).
[11]J. Schefer, P. Fischer, H. Heer, A. Isacson, M. Koch, and R.

Thut, Nucl. Instrum. Methods Phys. Res. Sect. A **288**, 477 (1990).
[12]H. M. Rietveld, J. Appl. Crystallogr. **2**, 65 (1969); A. W. Hewat, UKAEA Harwell report R7350 (1973).
[13]V. F. Sears, *Methods of Experimental Physics,* edited by K. Sköld and D. L. Price (Academic, London, 1986), Vol. 23A, p. 599.
[14]A. J. Freeman, J. P. Desclaux, G. H. Lander, and J. Faber, Phys. Rev. B **13**, 1168 (1976).
[15]L. Keller, Ph.D. thesis, Eidgenössische Technische Hochschule, Zürich (1994).
[16]M. Steiner, J. Villain, and C. G. Windsor, Adv. Phys. **25**, 87 (1976).
[17]L. Onsager, Phys. Rev. **65**, 117 (1944).
[18]A. Bienenstock, J. Appl. Phys. **37**, 1459 (1966).
[19]K. W. H. Stevens, Proc. Phys. Soc. London Sect. A **65**, 209 (1952).
[20]M. T. Hutchings, in *Solid State Physics: Advances in Research and Applications,* edited by F. Seitz and D. Turnbull (Academic, New York, 1964), Vol. 10, p. 227.
[21]K. Krämer (unpublished).
[22]K. R. Lea, M. J. M. Leask, and W. P. Wolf, J. Phys. Chem. Solids **23**, 1381 (1962).